\



Perpendicular magnetic anisotropy of Pd/Co_2MnSi/$NiFe_2O_4$/Pd multilayers on F-mica substrates

Qingwang Bai(白青旺), Bin Guo(郭斌), Qin Yin(尹钦), and Shuyun Wang(王书运)†

Citation: Chin. Phys. B, 2022, 31 (**1**): 017501. DOI: 10.1088/1674-1056/ac20cc
Journal homepage: http://cpb.iphy.ac.cn; http://iopscience.iop.org/cpb

What follows is a list of articles you may be interested in

Magnetic anisotropy manipulation and interfacial coupling in $Sm_3Fe_5O_{12}$ films and CoFe/$Sm_3Fe_5O_{12}$ heterostructures

Lei Shen(沈磊), Guanjie Wu(武冠杰), Tao Sun(孙韬), Zhi Meng(孟智), Chun Zhou(周春), Wenyi Liu(刘文怡), Kang Qiu(邱康), Zongwei Ma(马宗伟), Haoliang Huang(黄浩亮), Yalin Lu(陆亚林), Zongzhi Zhang(张宗芝), and Zhigao Sheng(盛志高)
Chin. Phys. B, 2021, 30 (**12**): 127502. DOI: 10.1088/1674-1056/ac0040

Optimized growth of compensated ferrimagnetic insulator $Gd_3Fe_5O_{12}$ with a perpendicular magnetic anisotropy

Heng-An Zhou(周恒安), Li Cai(蔡立), Teng Xu(许腾), Yonggang Zhao(赵永刚), and Wanjun Jiang(江万军)
Chin. Phys. B, 2021, 30 (**9**): 097503. DOI: 10.1088/1674-1056/ac0db0

Magnetic dynamics of two-dimensional itinerant ferromagnet Fe_3GeTe_2

Lijun Ni(倪丽君), Zhendong Chen(陈振东), Wei Li(李威), Xianyang Lu(陆显扬), Yu Yan(严羽), Longlong Zhang(张龙龙), Chunjie Yan(晏春杰), Yang Chen(陈阳), Yaoyu Gu(顾耀玉), Yao Li(黎遥), Rong Zhang(张荣), Ya Zhai(翟亚), Ronghua Liu(刘荣华), Yi Yang(杨燚), and Yongbing Xu(徐永兵)
Chin. Phys. B, 2021, 30 (**9**): 097501. DOI: 10.1088/1674-1056/ac0e25

Magnetic characterization of a thin Co_2MnSi/$L1_0$–MnGa synthetic antiferromagnetic bilayer prepared by MBE

Shan Li(黎姗), Jun Lu(鲁军)†, Si-Wei Mao(毛思玮), Da-Hai Wei(魏大海), and Jian-Hua Zhao(赵建华)
Chin. Phys. B, 2020, 29 (**10**): 107501. DOI: 10.1088/1674-1056/ab99ac

Magnetic properties of $L1_0$ FePt thin film influenced byrecoverable strains stemmed from the polarization of $Pb(Mg_{1/3}Nb_{2/3})O_3$-$PbTiO_3$ substrate

Li-Wang Liu(刘立旺), Cheng-Chao Hu(胡成超), Ye-Chuan Xu(徐野川), Hou-Bing Huang(黄厚兵), Jiang-Wei Cao(曹江伟), Linyun Liang(梁林云), Wei-Feng Rao(饶伟锋)
Chin. Phys. B, 2018, 27 (**7**): 077503. DOI: 10.1088/1674-1056/27/7/077503

Perpendicular magnetic anisotropy of Pd/Co_2MnSi/$NiFe_2O_4$/Pd multilayers on F-mica substrates

Qingwang Bai(白青旺), Bin Guo(郭斌), Qin Yin(尹钦), and Shuyun Wang(王书运)†

School of Physics and Electronics, Shandong Normal University, Ji'nan 250358, *China*

(Received 5 August 2021; revised manuscript received 19 August 2021; accepted manuscript online 25 August 2021)

Pd/Co_2MnSi (CMS)/$NiFe_2O_4$ (NFO)/Pd multilayers were fabricated on F-mica substrate by magnetron sputtering. The best PMA performance of the multilayer structure Pd(3 nm)/CMS(5 nm)/NFO(0.8 nm)/Pd(3 nm) was obtained by adjusting the thickness of the CMS and NFO layers. F-mica substrate has a flatter surface than glass and Si/SiO_2 substrate. The magnetic anisotropy energy density ($K_{\rm eff}$) of the sample deposited on F-mica substrates is 0.6711 Merg/cm^3 (1 erg = 10^{-7} J), which is about 30% higher than that of the multilayer films deposited on glass (0.475 Merg/cm^3) and Si/SiO_2 (0.511 Merg/cm^3) substrates, and the $R_{\rm Hall}$ and $H_{\rm C}$ are also significantly increased. In this study, the NFO layer prepared by sputtering in the high purity Ar environment was exposed to the high purity O_2 atmosphere for 5 min, which can effectively eliminate the oxygen loss and oxygen vacancy in NFO, ensuring enough Co–O orbital hybridization at the interface of CMS/NFO, and thus effectively improve the sample PMA.

Keywords: perpendicular magnetic anisotropy, Co_2MnSi, ferrimagnetics $NiFe_2O_4$

PACS: 75.30.Gw，75.50.Cc，75.50.Gg **DOI:** 10.1088/1674-1056/ac20cc

1. Introduction

Magnetic tunneling junctions (MTJs) with perpendicular magnetic anisotropy (PMA) have high enough thermal stability and low critical switching current in magnetoresistive random access memory (MRAM), so magnetic recording materials with PMA have become one of the research hot spots in recent years.[1–3] Over the years, Co-based multilayer films (Co/Pd and Co/Pt), rare-earth and transition metal alloys (GdFeCo) and L1 ordered alloys (CoPt and FePt) have been studied in depth.[4–6] However, these materials have some limitations such as inadequate chemical or thermal stability and low spin polarizability.[7,8] Full Hessler alloy Co_2MnSi (CMS) has a series of advantages, such as good thermal stability, nearly 100% spin polarizability, high Curie temperature $T_{\rm c}$ ($\sim$ 1000 K), very low Gilbert damping constant α ($\sim$ 0.001), and large tunneling magnetoresistance (TMR). So it has attracted widespread attention from people in recent years.[9,10] CMS is a promising candidate material for magnetic recording.[11–13]

Studies have shown that strong PMA can be induced by the interface effect between ferromagnetic metals (FM) and metal oxides (OX), such as CoFeB/MgO, Co/MgO, and Co_2MnSi/NiO structures.[14–16] Moreover, spinel oxides, such as $MgAl_2O_4$ and $MgGa_2O_4$, can further improve the performance of MTJs when used as a tunnel barrier due to their small lattice mismatch with typical FM electrodes.[17,18] $NiFe_2O_4$ (NFO) is a typical ferromagnetic spinel oxide with high magnetic ordering temperature and high saturation susceptibility. It is a very attractive candidate material for spintronic devices.[19] In particular, NFO has been successfully used as a spin-filtering tunnel barrier with a spin filtering efficiency of up to 22% at low temperatures.[20] Therefore, using NFO as a tunneling barrier for MTJs will increase the electron polarizability and thus increase TMR. Li *et al.* predicted by theoretical calculation that NFO could induce large PMA.[21] So far, there have been few studies on the PMA of CMS/NFO heterostructures.

In addition, mica substrate has a flat and inert surface, which is very conducive to the epitaxial growth of two-dimensional materials. In recent years, many researchers have grown high-quality thin film materials on mica substrates.[22–24] However, in the field of magnetic thin film materials, there are few studies on preparing of samples on mica substrates. In this paper, the magnetic properties of Pd/CMS/NFO/Pd multilayers deposited on mica substrates by sputtering were compared with those deposited on glass substrates and Si/SiO_2 substrates.

2. Experiments

All samples in this experiment were deposited on fluorphlogopite mica (F-mica) substrates at 350 °C by magnetron sputtering unless otherwise specified. The background vacuum before deposition is better than 6×10^{-4} Pa. The substrate is rotated at 15 rpm to ensure the uniformity of sputtering deposition. The structure and preparation details of this series of samples are shown in Table 1 (symbols or numbers in parentheses indicate film thickness in nanometers). In this experiment, all NFO layers prepared by sputtering were soon exposed to an oxygen atmosphere of 0.5 Pa for 5 min unless

†Corresponding author. E-mail: wangshuyun65@163.com

© 2022 Chinese Physical Society and IOP Publishing Ltd

otherwise stated. In this paper, the sputtering rate of each target material is measured by mass weighing method, and the required thickness of film is obtained by controlling the sputtering time. The sputtering parameters of all the targets are shown in Table 2.

The magnetic properties of the samples were measured by an alternating gradient magnetometer AGM: MicroMag 2900. The Hall curve of the samples was measured by four-probe method. The surface morphology of different substrates was measured by atomic force microscopy AFM:BY-5000.

Table 1. Series of samples and corresponding experimental variables.

Sample structure	Experiment variables
Pd(3)/CMS(t_{CMS})/NFO(0.8)/Pd(3)	CMS thickness: $t_{CMS} = 3, 4, 5, 6, 7, 8, 9$ nm
Pd(3)/CMS(5)/NFO(t_{NFO})/Pd(3)	NFO thickness: $t_{NFO} = 0, 0.4, 0.6, 0.8, 1, 1.4, 1.6$ nm
Pd(3)/CMS(5)/NFO(0.8)/Pd(3)	exposure time to oxygen atmosphere after sputtering NFO layer: $T_{O_2} = 0, 1, 3, 5, 10, 30$ min
Pd(3)/CMS(5)/NFO(0.8)/Pd(3)	substrate: F-mica substrate, glass substrate, Si/SiO_2 substrate

Table 2. Sputtering parameters for all targets.

Target	Power source (DC/RF)	Pressure (Pa)	Power (W)	Gas flow (sccm)
Pd	DC	0.5	15	Ar20
CMS	DC	0.5	30	Ar20
NFO	RF	0.5	40	Ar20

3. Results and discussion

3.1. Effects of the thickness of CMS layer on PMA

Figure 1(a) shows the Hall loops of a series of Pd(3)/CMS(t_{CMS})/NFO(0.8)/Pd(3) multilayers with different CMS thicknesses. Figure 1(b) shows the coercivity field (H_C) and Hall resistance (R_{Hall}) as functions of the thickness of the CMS layer. When $t_{CMS} = 3$ nm, the films do not exhibit PMA, because the relatively thin CMS layer cannot form strong interface effect with Pd and NFO to overcome the demagnetization energy.[25] The squareness of Hall loops becomes better and R_{Hall} increases with the increase of CMS thickness. The close to 1 of squareness and large R_{Hall} were observed at the $t_{CMS} = 5$ nm, indicating that the sample has a strong PMA. As the thickness of CMS continues to increase, the demagnetization energy of the sample increases, so that the R_{Hall} decreases gradually. When $t_{CMS} = 9$ nm, the PMA is disappear, which is attributed to the interfacial anisotropy energy cannot overcome the demagnetization energy.[15,16] H_C of the samples decreases slightly with the increase of CMS thickness, which can be found in Fig. 1(b).

Figure 1(c) show the in-plane and out-of-plane hysteresis loops of Pd(3)/CMS(5)/NFO(0.8)/Pd(3). A typical square out-of-plane hysteresis loop is observed, with 100% remanence, and a coercive field of about 425.36 Oe (1 Oe=79.5775 A/m). These data are basically consistent with those of Hall loops. The magnetic anisotropy energy density (K_{eff}) value can be estimated from the area difference between the magnetization curve of the in-plane and that of out-of-plane: $K_{eff} = \int [M_\perp - M_{\parallel}] \mathrm{d}H$, where $M_\perp$ is the out-of-plane magnetization, $M_{\parallel}$ is the in-plane magnetization. The sample K_{eff} value of 0.6711 Merg/cm^3 was calculated, reflecting the excellent PMA performance of the sample.[14]

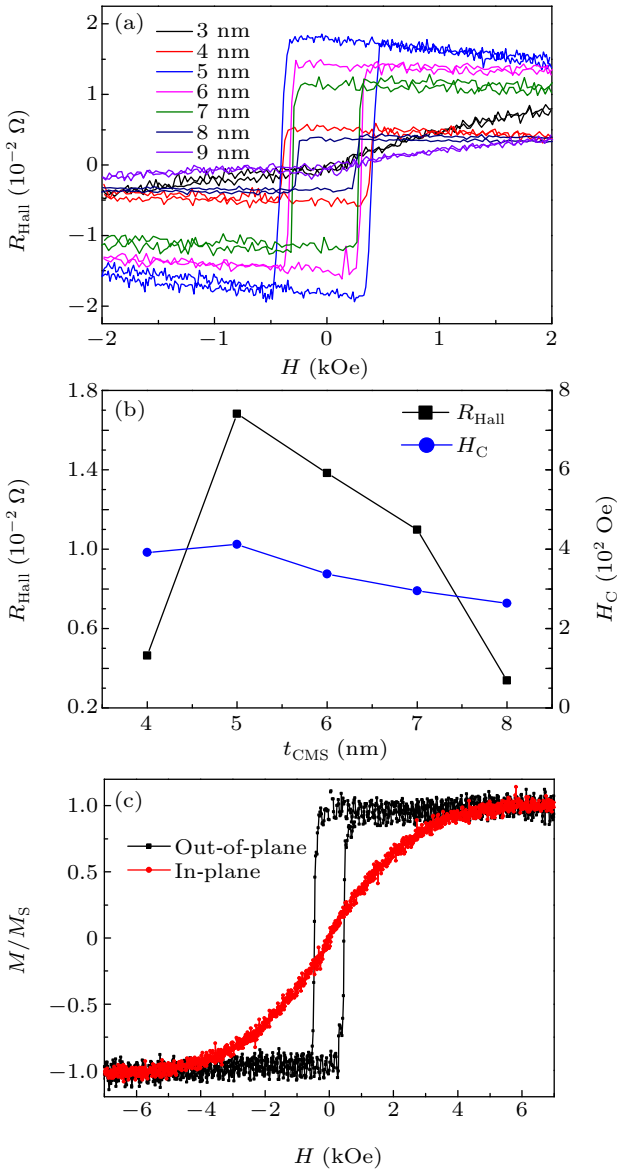


Fig. 1. (a) Hall loops of Pd (3)/CMS(t_{CMS})/NFO(0.8)/Pd(3) under different t_{CMS}, (b) t_{CMS} dependencies of R_{Hall} (black) and H_C (blue), (c) in-plane and out-of-plane hysteresis loops of Pd(3)/CMS(5)/NFO(0.8)/Pd(3).

3.2. Effect of NFO thickness on PMA

Hall loops of a series of Pd(3)/CMS(5)/NFO(t_{NFO})/Pd(3) multilayers with different NFO thicknesses are shown in Fig. 2(a). In general, the PMA of FM/OX multilay-

ers is strongly affected by the degree of oxidation at the interface.[26,27] The thickness of the oxide layer is a key factor affecting the oxidation state of the interface, so appropriate oxide layer thickness is crucial for obtaining strong PMA.[14–16,28] When $t_{NFO} = 0.2$ nm or 1.4 nm, the CMS/NFO interface was in the state of under-oxidation and overoxidation, respectively, the sample is displayed in-plane magnetic easy axis. When $t_{NFO} = 0.8$ nm, the sample has excellent Hall loops squareness and large R_{Hall}, which reflects the sample has strong PMA. The t_{NFO} dependence of H_C and R_{Hall} were basically consistent as observed in Fig. 2(b), suggesting that the H_C of the sample with strong PMA was relatively large only under the change of t_{NFO}. Similar phenomena have been observed in CMS/MgO, CMS/MAO and other structures.[28,29] In conclusion, when the thickness of NFO layer was 0.8 nm, the optimal interfacial oxidation degree of FM/OX interface was obtained, and PMA of the sample is the strongest.

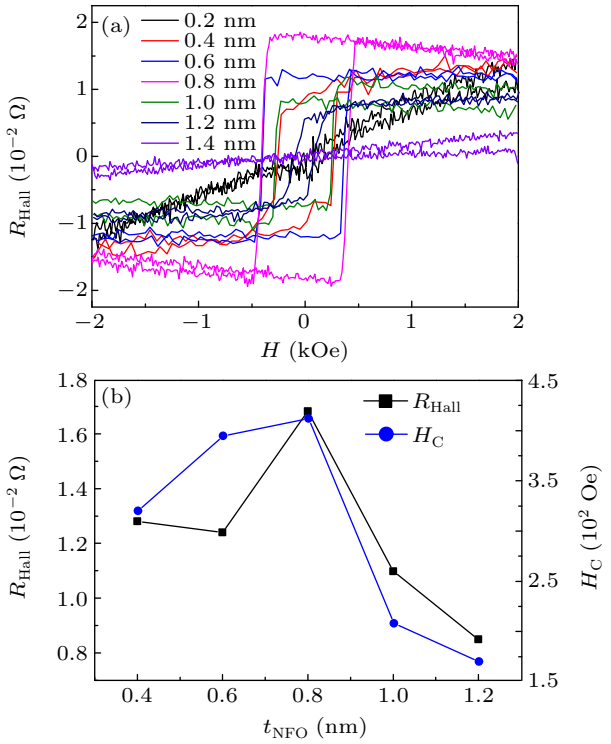


Fig. 2. (a) Hall loops for Pd(3)/CMS(5)/NFO(t_{NFO})/Pd(3) with various t_{NFO} from 0.2 nm to 1.4 nm, (b) R_{Hall} (black) and H_C (blue) dependence on t_{NFO}.

3.3. Effect of T_{O_2} on PMA

It is well known that PMA is mainly originated from the orbital hybridization of Co-3d and O-2p at the interface of CMS/OX multilayers.[29,30] During the preparation of oxide layer, a certain proportion of O_2 is usually injected into the sputtering gas in order to reduce oxygen loss and oxygen vacancy in the oxide layer.[14–16] However, the ferromagnetic layer will be overoxidized if too much oxygen is introduced. Therefore, in this experiment, the oxide layer was sputtered in high purity Ar environment, and then exposed to high purity O_2 atmosphere, so that the sputtered oxide layer was sufficient oxidized to eliminate oxygen loss and oxygen vacancy. Figure 3(a) shows the Hall loops of a series of Pd(3)/CMS(5)/NFO(0.8)/Pd(3) multilayers with different T_{O_2} (exposure time to oxygen atmosphere after sputtering NFO layer). Figure 3(b) shows the R_{Hall} and H_C dependence of T_{O_2}. When $T_{O_2} = 0$ min, the Hall loops squareness is poor and R_{Hall} is small, indicating that the PMA of the sample is weak. This is because the oxygen loss and the oxygen vacancy in the NFO lead to insufficient Co–O orbital hybridization at the CMS/NFO interface, which resulting in a weak interface effect of CMS/NFO.[17,31] The close to 1 of squareness and large R_{Hall} can be observed at the $T_{O_2} \geq 5$ min, showing that the sample exhibited strong PMA. The R_{Hall} and H_C of the sample remain basically unchanged as T_{O_2} continues to increase. To sum up, oxygen loss and oxygen vacancy in NFO can be basically eliminated at $T_{O_2} \geq 5$ min, and no overoxidation will occur at the CMS/NOF interface.

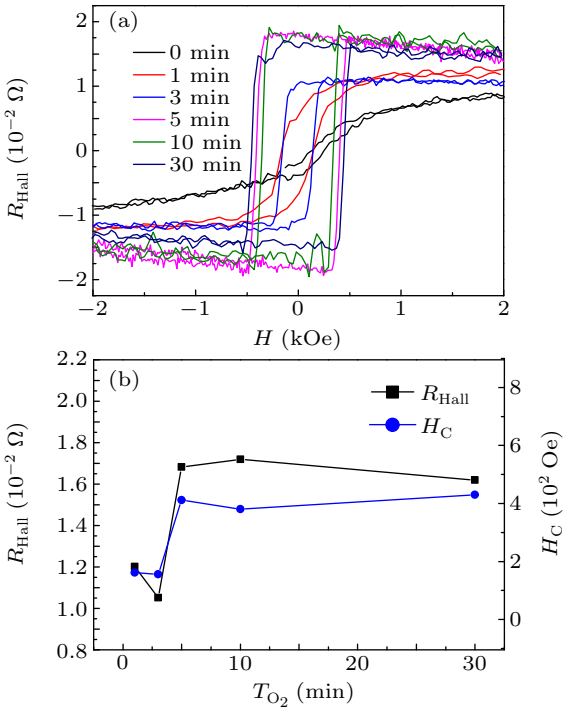


Fig. 3. (a) Hall loops for Pd(3)/CMS(5)/NFO(0.8)/Pd(3) with various T_{O_2} from 0 min to 30 min, (b) R_{Hall} (black) and H_C (blue) dependence on T_{O_2}.

3.4. Effect of substrates on PMA

The Hall loops and the in-plane and the out-of-plane hysteresis loops of a series of Pd(3)/CMS(5)/NFO(0.8)/Pd(3) multilayers deposited on different substrates are shown in Fig. 4. The samples deposited on F-mica substrates have larger R_{Hall} and H_C compared with those deposited on glass and Si/SiO_2 substrates. Suitable H_C can make the magnetic properties of thin films more stable and facilitate the miniaturization of devices.[32] By calculating the K_{eff} value of these samples, it was found that the K_{eff} value of the sample de-

posited on the F-mica substrate is 0.6711 Merg/cm^3, which was about 30% larger than that of the samples deposited on the glass (0.475 Merg/cm^3) and Si/SiO$_2$ (0.511 Merg/cm^3) substrate. The surface morphologies of three different substrates were observed by AFM, as shown in Fig. 5. As can be seen from the figure, F-mica substrate has a flatter surface than glass and Si/SiO$_2$ substrate. The roughness of F-mica substrate is 0.083 nm, which is only one third of that of glass substrate (0.231 nm) or Si/SiO$_2$ substrate (0.243 nm). The flatness of the substrate provides conditions for the deposition of high quality films and interfaces on it, which is more conducive to improving the PMA of multilayers.[22–24,33]

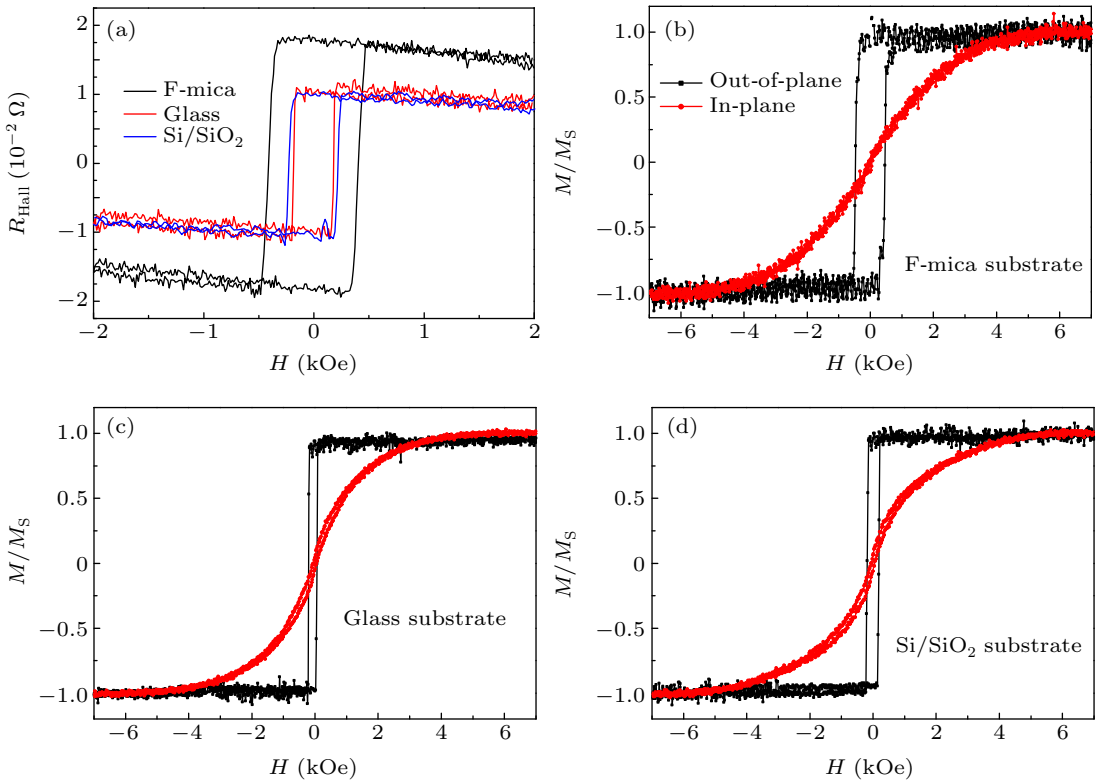


Fig. 4. (a) Hall loops and (b)–(d) in-plane and out-plane M–H loops of Pd(3)/CMS(5)/NFO(0.8)/Pd(3) multilayers deposited on different substrates.

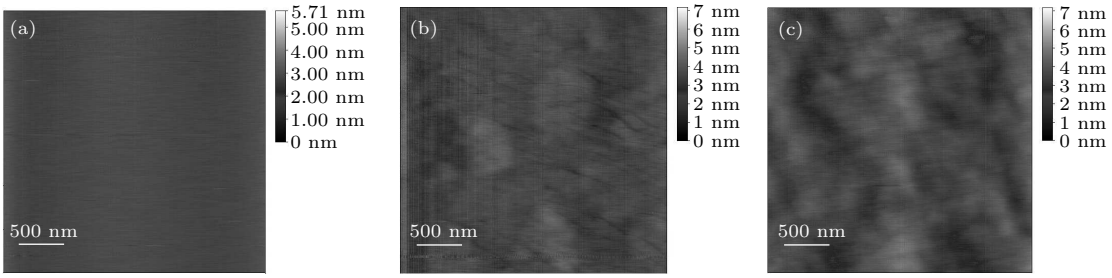


Fig. 5. Surface morphologies of (a) F-mica substrates, (b) glass substrates, and (c) Si/SiO$_2$ substrates.

4. Conclusion

A series of Pd (3)/CMS(t_{CMS})/NFO(t_{NFO})/Pd(3) multilayers were fabricated on F-mica substrates by magnetron sputtering. The Pd(3)/CMS(5)/NFO(0.8)/Pd(3) multilayer structure with the best PMA performance was obtained by adjusting the thickness of CMS and NFO, and the sample K_{eff} value was 0.6711 Merg/cm^3. In this study, the NFO layer fabricated by sputtering in high purity Ar environment was exposed to high purity O$_2$ atmosphere for 5 min, which could effectively eliminate the oxygen loss and oxygen vacancy in NFO, ensuring enough Co–O orbital hybridization at the CMS/NFO interface, and thus effectively improve the sample PMA. Compared with the samples deposited on glass and Si/SiO$_2$ substrates, the multilayers deposited on F-mica substrates have larger R_{Hall} and H_C, and the K_{eff} value is also significantly increased. The K_{eff} value of the Pd/CMS/NFO/Pd multilayers deposited on the F-mica substrate is 0.6711 Merg/cm^3, which is about 30% larger than that of the samples deposited on the glass (0.475 Merg/cm^3) and Si/SiO$_2$ (0.511 Merg/cm^3) substrates. In the following work, we will try to applying a magnetic field during the film deposition to continue to enhance the PMA of the multilayers.[34]

Acknowledgment

Project supported by the Shandong Provincial Natural Science Foundation, China (Grant No. ZR2018MEM004).

References

[1] Ikeda S, Miura K, Yamamoto H, Mizunuma K, Gan H D, Endo M, Kanai S, Hayakawa J, Matsukura F and Ohno H 2010 *Nat. Mater.* **9** 721
[2] Wang J, Tu H Q, Liang J, Zhai Y, Liu R B, Yuan Y, Huang L A, Liu T Y, Liu B, Meng H, You B, Zhang W, Xu Y B and Du J 2020 *Chin. Phys. B* **29** 107503
[3] Feng J F, Kurt H, Venkatesan M and Coey J M D 2012 *Thin Solid Films* **520** 7173
[4] Dong K F, Deng J Y, Jin F, Mo W Q, Song J L and Chen J S 2018 *J. Alloys Compd.* **730** 234
[5] Davydenko A V, Kozlov A G, Ognev A V, Stebliy M E, Samardak A S, Ermakov K S, Kolesnikov A G and Chebotkevich L A 2017 *Phys. Rev. B* **95** 064430
[6] Ding M and Poon S J 2013 *J. Magn. Magn. Mater.* **339** 51
[7] Kim G, Sakuraba Y, Oogane M, Ando Y and Miyazaki T 2008 *Appl. Phys. Lett.* **92** 172502
[8] Bandiera S, Sousa R R, Rodmacq BB and Dieny B 2011 *IEEE Magn. Lett.* **2** 3000504
[9] Jiang S, Nazir S and Yang K 2020 *Phys. Rev. B* **101** 134405
[10] Qiao S Z, Zhang J, Qin Y F, Hao R R, Zhong H, Zhu D P, Kang Y, Kang S S, Yu S Y, Han G B, Yan S S and Mei L M 2015 *Chin. Phys. Lett.* **32** 057601
[11] Mao S, Lu J, Zhao X, Wang X, Wei D, Liu J, Xia J and Zhao J 2017 *Sci. Rep.* **7** 43064
[12] Bai Q, Jiang J, Guo B, Cao W, Xiu X and Wang S 2021 *J. Magn. Magn. Mater.* **539** 168335
[13] Fu H, You C, Li Y, Wang K and Tian N 2016 *J. Phys. D: Appl. Phys.* **49** 195001
[14] Akyol M 2019 *J. Supercond. Novel Magn.* **32** 457
[15] Yu G H, Peng W L and Zhang J Y 2017 *Rare Metals* **36** 155
[16] Jiang J, Xiu X, Wen K, Cao W, He Y and Wang S 2020 *J. Magn. Magn. Mater.* **505** 166709
[17] Sukegawa H, Hadorn JP, Wen Z, Ohkubo T, Mitani S and Hono K 2017 *Appl. Phys. Lett.* **110** 112403
[18] Mertens S, Couet S, Carpenter R, Swerts J, Crotti D and Kar G S 2021 *Appl. Phys. Lett.* **118** 172402
[19] Anoop Baby K B, Ugendar K, Subrahmanyam A and Markandeyulu G 2019 *IEEE Trans. Magn.* **55** 1
[20] Lüders U, Bibes M, Bouzehouane K, Jacquet E, Contour J P, Fusil S, Bobo J F, Fontcuberta J, Barthélémy A and Fert A 2006 *Appl. Phys. Lett.* **88** 082505
[21] Li F, Yang B, Zhang J, Han X and Yan Y 2020 *Phys. Chem. Chem. Phys.* **22** 716
[22] Cui F, Wang C, Li X, Wang G, Liu K, Yang Z, Feng Q, Liang X, Zhang Z, Liu S, Lei Z, Liu Z, Xu H and Zhang J 2016 *Adv. Mater.* **28** 5019
[23] Liu Y, Tang M, Meng M, Wang M, Wu J, Yin J, Zhou Y, Guo Y, Tan C, Dang W, Huang S, Xu H Q, Wang Y and Peng H 2017 *Small* **13** 1603572
[24] Li B, Ding L, Gui P, Liu N, Yue Y, Chen Z, Song Z, Wen J, Lei H, Zhu Z, Wang X, Su M, Liao L, Gao Y, Zhang D and Fang G 2019 *Adv. Mater. Interfaces* **6** 1901156
[25] Fu H R, Ma L, Tian N, You C Y and Wang K 2018 *AIP Adv.* **8** 055804
[26] Feng C, Wang S, Yin L, Li X, Yao M, Yang F, Tang X, Wang L, Mi W and Yu G 2018 *Adv. Funct. Mater.* **28** 1803335
[27] L S, M M R, D P, V P, Ikeda H and Therese H A 2018 *Mater. Res. Bull.* **107** 118
[28] Saravanan L, Raja MM, Prabhu D, Pandiyarasan V, Ikeda H and Therese HA 2018 *J. Magn. Magn. Mater.* **454** 267
[29] Peng S, Wang M, Yang H, Zeng L, Nan J, Zhou J, Zhang Y, Hallal A, Chshiev M, Wang K L, Zhang Q and Zhao W 2015 *Sci. Rep.* **5** 18173
[30] Scheike T, Sukegawa H, Inomata K, Ohkubo T, Hono K and Mitani S 2016 *Appl. Phys. Express* **9** 053004
[31] Wen K, Xiu X, Jiang J, He Y, Huang F and Wang S 2019 *J. Phys. D: Appl. Phys.* **52** 485005
[32] Moser A, Takano K, Margulies D T, Albrecht M, Sonobe Y, Ikeda Y, Sun S and Fullerton E E 2002 *J. Phys. D: Appl. Phys.* **35** R157
[33] Xu X, Nian X, Li B, Chen X, Liu S and Ju H 2017 *Integrated Ferroelectrics* **180** 77
[34] Xu X L, Huang Q M, Feng G N, Han G, Guo Q X, Xiong X D, He X, Luo J F, Wang R M, Feng C and Yu G H 2020 *Rare Metals* **40** 975